Chemistry & Biology, Vol. 11, 337–345, March, 2004, ©2004 Elsevier Science Ltd. All rights reserved. DOI 10.1016/j.chembiol.2004.02.023

Small Molecule Inhibitors of Mucin-Type *O*-Linked Glycosylation from a Uridine-Based Library

Howard C. Hang,[1,5] Chong Yu,[1,5] Kelly G. Ten Hagen,[4] E Tian,[4] Katharine A. Winans,[1,6] Lawrence A. Tabak,[4] and Carolyn R. Bertozzi[1,2,3,*]

[1]Department of Chemistry
[2]Department of Molecular and Cell Biology
[3]Howard Hughes Medical Institute
Center for New Directions in Organic Synthesis
University of California, Berkeley
Berkeley, California 94720
[4]Section of Biological Chemistry
NIDDK
National Institutes of Health
Bethesda, Maryland 20892

Summary

The polypeptide *N*-acetyl-α-galactosaminyltransferases (ppGalNAcTs, also abbreviated ppGaNTases) initiate mucin-type *O*-linked glycosylation and therefore play pivotal roles in cell-cell communication and protection of tissues. In order to develop new tools for studying mucin-type *O*-linked glycosylation, we screened a 1338 member uridine-based library to identify small molecule inhibitors of ppGalNAcTs. Using a high-throughput enzyme-linked lectin assay (ELLA), two inhibitors of murine ppGalNAcT-1 ($K_i \sim 8$ μM) were identified that also inhibit several other members of the family. The compounds did not inhibit other mammalian glycosyltransferases or nucleotide sugar utilizing enzymes, suggesting selectivity for the ppGalNAcTs. Treatment of cells with the compounds abrogated mucin-type *O*-linked glycosylation but not *N*-linked glycosylation and also induced apoptosis. These uridine analogs represent the first generation of chemical tools to study the functions of mucin-type *O*-linked glycosylation.

Introduction

Protein glycosylation is important for a variety of cellular events such as protein trafficking and cell-cell interactions [1]. There are two major forms of protein glycosylation, *N*-linked and *O*-linked, distinguished by their glycosidic linkages to amino acid side chains. Mucin-type *O*-linked glycosylation (hereafter, all references to *O*-linked glycosylation refer to the mucin-type) is the dominant form of *O*-linked glycosylation in higher eurkaryotes, characterized by an *N*-acetyl-α-galactosamine (GalNAc) residue attached to the hydroxyl group of serine or threonine side chains (Figure 1) [2]. The biosynthesis of *O*-linked glycans is initiated by the family of polypeptide *N*-acetyl-α-galactosaminyltransferases (ppGalNAcTs), which transfer GalNAc from uridine diphosphate *N*-acetyl-α-galactosamine (UDP-GalNAc) onto proteins trafficking through the Golgi compartment (Figure 1) [3]. Elaboration of the core glycopeptide, termed the Tn-antigen, by downstream glycosyltransferases affords more complex glycan structures [4]. These *O*-linked glycans are thought to play critical roles in lubrication and protection of tissues [5–8], leukocyte homing [9], the immune response [10], and the metastasis of tumor cells [11].

While much is known about the functions of *N*-linked glycans [12, 13], progress toward understanding *O*-linked glycosylation has been hindered by the large number of ppGalNAcT isoforms present in vertebrate genomes (~24 in human) [3]. To date, 21 putative ppGalNAcTs have been cloned from various organisms [14–33], all of which have been biochemically characterized with the exception of ppGalNAcT-8 [24]. Transcript analysis has revealed differential tissue distribution and temporal regulation of ppGalNAcT expression during development and pregnancy [34, 35]. Targeted gene deletion of ppGalNAcT-1, -4, -5, or -13 in mice demonstrate no apparent phenotypes with respect to development, fertility, and immune function, suggesting functional redundancy or compensatory regulation amongst the ppGalNAcT family members [3]. However, recent studies of *D. melanogaster* mutants have shown that one ppGalNAcT, pgant35A, is essential for development [27, 28].

Studies of *O*-linked glycoprotein biosynthesis are further complicated by the overlapping peptide substrate specificities exhibited by the ppGalNAcT family in vitro and in vivo [3, 36, 37]. The identification of ppGalNAcTs that specifically recognize α-GalNAc-modified glycopeptides has enabled further subclassification of the family into peptide and glycopeptide transferases [22, 23, 26]. In contrast to *N*-linked glycosylation, where a single oligosaccharyl transferase catalyzes the modification of asparagine residues within the consensus sequence Asn-Xaa-Ser/Thr [38], no consensus sequence for *O*-linked glycosylation has been identified. Computational algorithms developed to predict the likelihood of *O*-linked glycosylation from primary amino acid sequences have been useful for identifying mucin domains within a protein [39]. However, these semiempirical methods have limited accuracy for predicting glycosylation of specific residues and therefore still require experimental confirmation. Finally, structural studies of acceptor peptide substrates suggest that ppGalNAcTs may recognize β-turn-like motifs rather than primary amino acid sequence alone [40].

The discovery and design of inhibitors that target *N*-linked glycan biosynthesis and processing have greatly increased our appreciation of *N*-linked glycosylation [41–43]. In contrast, few chemical tools are available to address mucin-type *O*-linked glycosylation. Competitive substrate-based primers can be used to

*Correspondence: crb@berkeley.edu
[5]These authors contributed equally to this work.
[6]Present address: Department of Medicine, Division of Infectious Diseases and Geographic Medicine, Stanford University Medical Center, Stanford, California 94305.

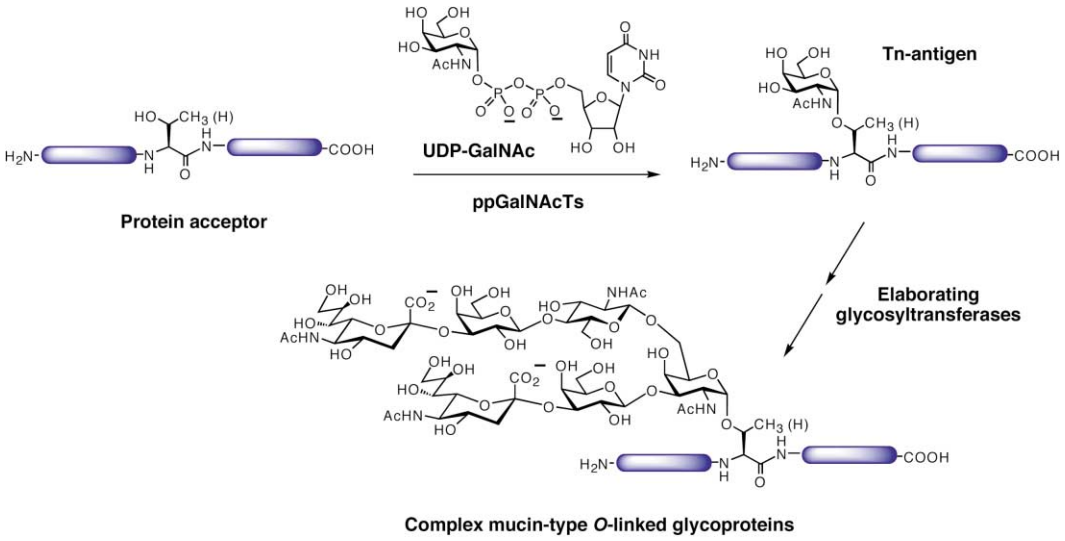

Figure 1. Initiation of Mucin-Type *O*-Linked Glycosylation by ppGalNAcTs and Elaboration into Complex *O*-Linked Glycans by Downstream Glycosyltransferases

inhibit the downstream elaboration of *O*-linked glycans in cells, affording truncated structures [44–48]. But these compounds do not affect the attachment of GalNAc to Ser or Thr. Inhibitors of the ppGalNAcTs that initiate *O*-linked glycosylation have not been reported and would be powerful tools to further our understanding of this fundamental posttranslational modification.

Here we report the discovery of ppGalNAcT inhibitors from a uridine-based library designed to target enzymes that utilize UDP-sugar substrates [49]. The library conserved the uridine moiety of the nucleotide sugar substrate, while replacing the sugar and diphosphate groups with drug-like diversity elements (Figure 2A). Three different linkers were utilized to couple the uridine component with a diverse array of 446 aldehydes via an oxime or hydrazone linkage (Figure 2B). This library has previously produced selective inhibitors of the human UDP-GlcNAc/GalNAc C_4-epimerase [49] and the mycobacterial UDP-galactopyranose-mutase [50]. Two compounds were identified from the library that inhibited all the ppGalNAcTs tested.

Results and Discussion

Development and Validation of a High-Throughput Assay for ppGalNAcTs

In order to screen the library in high-throughput format, we developed a nonradioactive enzyme-linked lectin assay (ELLA) for ppGalNAcTs. A schematic diagram of the assay is shown in Figure 3A. As an acceptor substrate, we chose the EA2 peptide (PTTDSTTPAPTTK), a fragment of rat submandibular mucin [51]. This peptide has been previously shown to be an efficient substrate for murine (m) ppGalNAcT-1 and is preferentially glycosylated at the fourth Thr residue from the N terminus (underlined) [26]. Biotinylation of EA2 allowed capture of (glyco)peptides onto 96-well NeutrAvidin-coated plates. The immobilized glycopeptide product could be detected using the α-GalNAc-specific lectin *Helix pomatia agglutinin* (HPA) [52] conjugated to horseradish peroxidase (HRP) after addition of a chromogenic HRP substrate.

In order to correlate the change in absorbance produced by HRP activity to the enzymatic activity of mppGalNAcT-1, a standard curve for the ELLA response was generated. Peptide **4** and glycopeptide **5**, biotinylated at the C terminus, were constructed by Fmoc-based solid-phase peptide synthesis using previously described methods (Figure 3B) [53]. Peptide **4** and glycopeptide **5** were combined at various percentages, captured on NeutrAvidin-coated 96-well microtiter plates, and detected using the HPA-HRP conjugate. The standard curve derived from this experiment correlates the percentage of NeutrAvidin sites occupied by the glycopeptide with the observed signal. The absolute quantity of immobilized glycopeptide can be determined based on the known binding capacity of the NeutrAvidin-coated plates (60 pmol/well). The standard curve showed a dose-dependent increase in signal over a range of 0%–15% **5** (Figure 3C). The signal reached a plateau at higher concentrations of **5**, which we attributed to saturation of lectin binding. The signal to noise ratio observed at 15% **5** (9 pmol) was 30-fold above background. Thus, the assay can readily detect low picomole amounts of the product from the ppGalNAcT reaction.

To validate the ELLA, we measured the kinetic parameters of mppGalNAcT-1 with UDP-GalNAc, EA2 peptide **4**, and UDP (details are provided in the Supplemental Data at http://www.chembiol.com/cgi/content/full/11/3/337/DC1). The K_M values of UDP-GalNAc and EA2 peptide **4** were determined to be 13.9 ± 1.8 μM and 48.0 ± 4.0 μM, respectively. The K_I value for the product UDP was 251.1 ± 78.0 μM. These values are similar to those

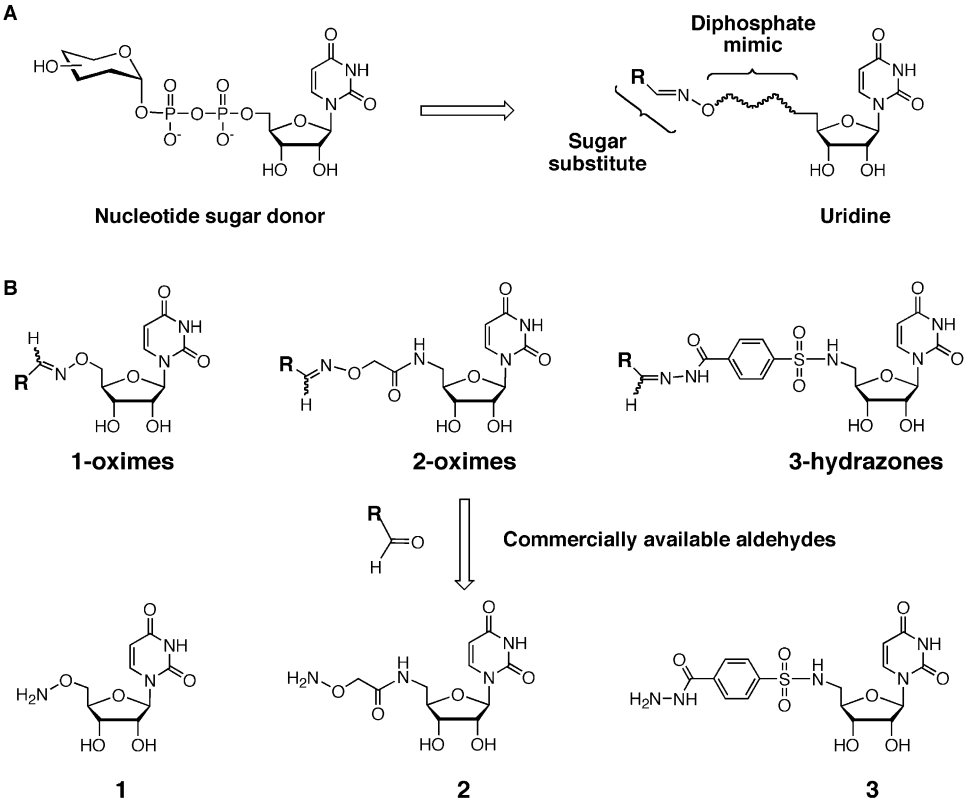

Figure 2. Uridine-Based Library

(A) Design of uridine-based library as nucleotide sugar mimics.

(B) Retrosynthesis of the uridine-based library. Compounds are numbered according to the uridine linker (**1**, **2**, and **3**) followed by the aldehyde (i.e., **1-299** or **1A-148A**; a complete list of aldehydes used in the library synthesis is provided in the Supplemental Data at http://www.chembiol.com/cgi/content/full/11/3/337/DC1).

previously determined using a radiolabel capture assay [20, 54].

Preliminary Screening of the Uridine-Based Library with mppGalNAcT-1

Using the ELLA, we performed preliminary screens of the 1338 member uridine-based library [49] at 40 μM with mppGalNAcT-1. From the preliminary screens, 32 initial hits displayed over 70% inhibition (Supplemental Data at http://www.chembiol.com/cgi/content/full/11/3/337/DC1). After rescreening these initial hits at 8 μM and resynthesis of confirmed hits, two mppGalNAcT-1 inhibitors **1-68A** and **2-68A** were identified (Figure 4A). The compounds comprised the same aldehyde component (**68A**) linked via an oxime to two different uridine scaffolds, **1** and **2**. Interestingly, the aldehyde component has a trihydroxybenzene functionality that resembles a monosaccharide.

Kinetic Analysis of Uridine-Based Inhibitors with mppGalNAcT-1

To determine the modes of **1-68A** and **2-68A** inhibition, we evaluated their inhibitory activity versus both substrates UDP-GalNAc and EA2 peptide **4**. The K_I values for **1-68A** and **2-68A** were determined to be 7.8 ± 0.1 μM and 7.8 ± 1.0 μM versus UDP-GalNAc, respectively (Figure 4B). Both compounds were competitive with respect to UDP-GalNAc and bind approximately 2-fold greater than UDP-GalNAc (K_M = 14 μM) and 30-fold greater than UDP (K_I = 250 μM). The compounds appeared to be noncompetitive with respect to EA2 peptide **4** (Supplemental Data at http://www.chembiol.com/cgi/content/full/11/3/337/DC1), a finding consistent with a random sequential mechanism reported by Wragg et al. [54].

To determine the contributions of the uridine and aldehyde components to binding, we assayed aldehyde **68A** and the parent aminooxy uridine analogs **1** and **2** for inhibitory activity. While uridine analogs **1** and **2** showed no inhibition at concentrations up to 400 μM (Supplemental Data at http://www.chembiol.com/cgi/content/full/11/3/337/DC1), compound **68A** exhibited competitive inhibitory activity with a K_I value of 34.3 ± 5.5 μM (Figure 4B). These data suggest that the binding affinity of **68A** was increased approximately 5-fold when coupled to uridine analogs **1** or **2**. It is interesting to note that the K_I values for compounds **1-68A** and **2-68A** are similar despite the different linker lengths, suggesting that the aldehyde component contributes significantly to binding. However, the adduct of aldehyde **68A** with

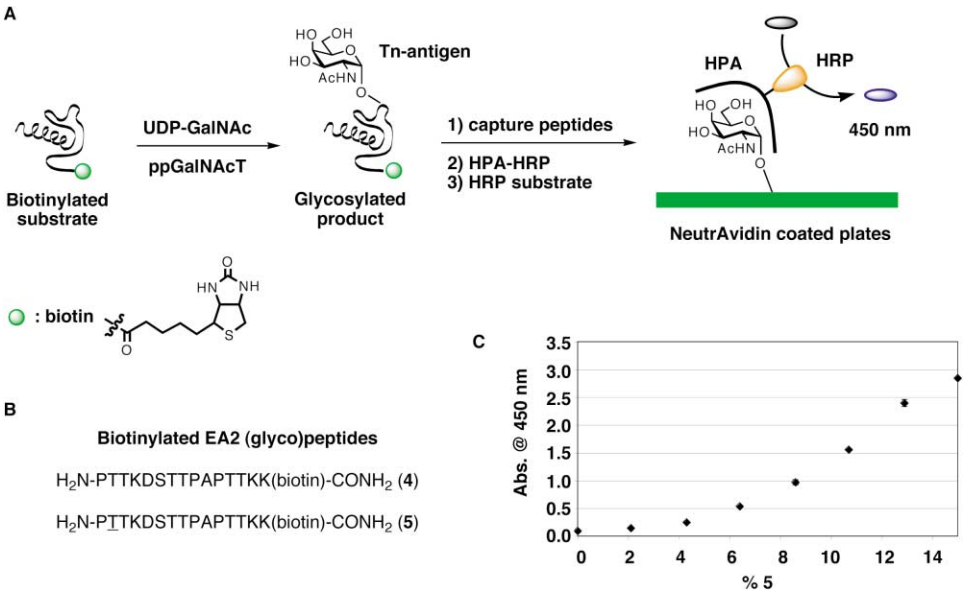

Figure 3. Enzyme-Linked Lectin Assay for Detecting ppGalNAcT Activity

(A) Schematic of the enzyme-linked lectin assay (ELLA).

(B) Biotinylated EA2 (glyco)peptides **4** and **5**. Sites of glycosylation bearing α-GalNAc are underlined. These were chosen based on an initial report that mppGalNAcT-1 modifies Thr2 with GalNAc [18]. It was later established that mppGalNAcT-1 modifies EA2 at Thr7 rather than Thr2 [26].

(C) ELLA standard curve generated with EA2 (glyco)peptides **4** and **5**. Each point on the graph represents the average of duplicates; error bars represent the high and low values.

uridine analog **3** (Figure 2), the longest of the three uridine linkers, showed no inhibitory activity in preliminary screens, suggesting the structure and/or length of the linker is a critical determinant of binding.

Inhibitory Activity against Other Related Enzymes

To evaluate the activities of compounds **1-68A** and **2-68A** with other ppGalNAcT isoforms, IC_{50} measurements for both compounds were performed with ppGalNAcTs 1–5, 7, 10, and 11 (Table 1, entries 1–8). Their inhibitory activities were similar with all ppGalNAcT isoforms tested, which suggests that **1-68A** and **2-68A** are broad-spectrum inhibitors of the ppGalNAcT family. To determine the inhibitory activities of the compounds among the broader family of glycosyltransferases, **1-68A** and **2-68A** were tested against bovine β1-4galactosyltransferase (β1-4GalT) [55] and porcine α1-3galactosyltransferase (α1-3GalT) [56], using a previously re-

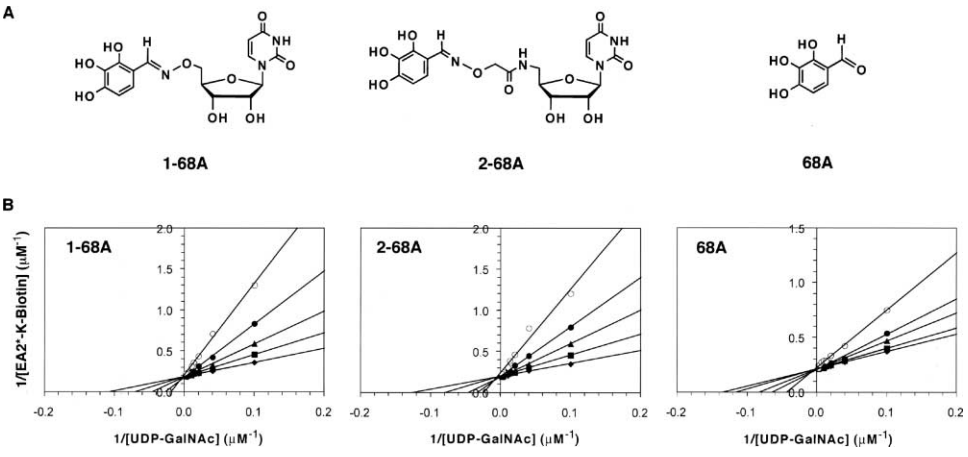

Figure 4. ppGalNAcT Inhibitors Identified from the Uridine-Based Library

(A) Structures of mppGalNAcT-1 inhibitors **1-68A** and **2-68A** and parent aldehyde **68A**.

(B) K_i measurements for **1-68A**, **2-68A**, and **68A** with respect to UDP-GalNAc, against mppGalNAcT-1. The concentration of EA2 peptide **4** was held constant at 50 μM while the concentration of UDP-GalNAc was varied from 25 to 400 μM. Inhibitor concentrations were varied from 6 to 48 μM. The various concentrations of inhibitor are represented by the following symbols: closed diamond = 0 μM, closed square = 6 μM, closed up triangle = 12 μM, closed circle = 24 μM, and open circle = 48 μM. Each point on the graph represents the average of duplicates; error bars represent the high and low values.

Table 1. IC_{50} Values for **1-68A** and **2-68A** with ppGalNAcTs 1–5, 7, 10, 11, β1-4GalT, and α1-3GalT

	2.1-68A (μM)	2.2-68A (μM)
mppGalNAcT-1	21 ± 1	24 ± 2
mppGalNAcT-2	15 ± 1	18 ± 2
mppGalNAcT-3	40 ± 2	38 ± 4
mppGalNAcT-4	30 ± 5	20 ± 5
rppGalNAcT-5	20 ± 2	26 ± 9
rppGalNAcT-7	22 ± 2	27 ± 2
rppGalNAcT-10	7 ± 1	6 ± 1
mppGalNAcT-11	39 ± 3	32 ± 3
β1-4GalT	>500	>500
α1-3GalT	>500	>500

The requirement of glycopeptides as substrates for ppGalNAcT-7 and -10 precluded the use of the ELLA, as both the substrate and product bind HPA-HRP. Thus, the radiolabel capture assay was employed to measure the IC_{50} values of **1-68A** and **2-68A** with ppGalNAcT-7 and -10 using MUC5AC** (GTTPSPVPTTSTTSAP) glycopeptide, previously shown to be substrate for both enzymes [22, 26]. IC_{50} values of **1-68A** and **2-68A** with ppGalNAcT-5 were performed with α-FLAG purified enzyme and radiolabel capture assay, due to low activity and stability of the crude enzyme. m, murine; r, rattus.

ported continuous colorimetric assay [57]. Neither compound was active against β1-4GalT or α1-3GalT at the highest concentration tested (500 μM) (Table 1, entries 9 and 10). While every UDP-sugar utilizing enzyme in the vertebrate genome has not been evaluated, the lack of inhibitory activity of **1-68A** and **2-68A** against β1-4GalT and α1-3GalT demonstrates that these compounds are not general inhibitors of inverting or retaining glycosyltransferases. It should also be noted that **1-68A** and **2-68A** were not identified in screens of the uridine-based library against the UDP-GlcNAc/GalNAc C_4-epimerase [49] or UDP-galactopyranose mutase [50]. Collectively, these observations suggest that **1-68A** and **2-68A** are selective inhibitors of the ppGalNAcT family and do not function as nonspecific inhibitors of UDP-sugar utilizing enzymes.

Evaluation of 1-68A and 2-68A Inhibitory Activity in Cells

Having demonstrated that **1-68A** and **2-68A** inhibit the ppGalNAcTs in vitro, we sought to evaluate their effects on *O*-linked glycosylation in cells. To directly monitor ppGalNAcT activities in cells, we chose Jurkat cells (human T cell lymphoma) that are known to produce the Tn-antigen (Figure 1) as their *O*-linked glycans [58]. Changes in Tn-antigen expression on the surface of Jurkat cells were monitored by HPA binding followed by flow cytometry analysis. Con A staining of *N*-linked glycans was used as a control for nonspecific inhibition of protein glycosylation [59]. As shown in Figure 5A, both **1-68A** and **2-68A** inhibited HPA staining of Jurkat cells in a dose-dependent manner (EC_{50} ~80 μM) with no significant effect on Con A staining. However, forward and side scatter analysis of the cells treated with either compound for 2 days indicated that a morphological change characteristic of apoptosis had occurred. Indeed, Annexin-V [60] staining of Jurkat cells treated with **1-68A** or **2-68A** confirmed the induction of apoptosis (Figure 5B) at inhibitor concentrations that also abrogate HPA staining.

It is possible that compounds **1-68A** and **2-68A** induce apoptosis independently of their effects on *O*-linked glycosylation and that changes in membrane architecture associated with the process affect lectin staining of cells. We therefore sought to address the effects of compounds known to induce apoptosis by glycosylation-independent mechanisms on lectin staining. Jurkat cells were treated with the pro-apoptotic drugs doxorubicin [61] and campothecin [62], which inhibit topoisomerases I and II, respectively, and evaluated for HPA, Con A, and Annexin V staining. As shown in Figures 5C and 5D, doxorubicin and campothecin induced Annexin V binding at levels comparable to **1-68A**. In contrast to **1-68A**, doxorubicin and campothecin reduced both HPA and Con A staining of Jurkat cells. Thus, the physiological changes associated with apoptosis alone cannot account for the selective reduction in HPA staining observed with **1-68A**. Moreover, it is unlikely that the effects of **1-68A** simply reflect a global disruption in metabolism, as one would expect a similar effect on *N*-linked glycan expression.

To determine if the inhibition of *O*-linked glycosylation and induction of apoptosis by **1-68A** and **2-68A** were specific to Jurkat cells, we evaluated the effects of **1-68A**

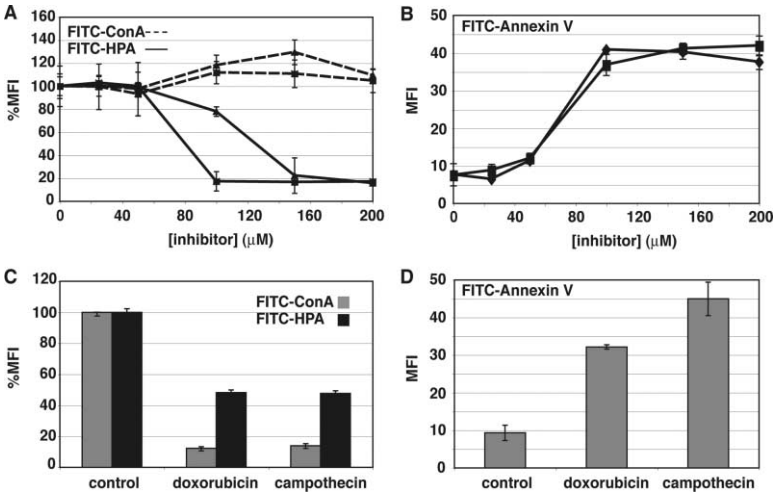

Figure 5. Effects of ppGalNAcT Inhibitors and the Apoptosis Inducers Doxorubicin and Campothecin in Jurkat Cells

(A) Lectin staining of *N*-linked (Con A, dashed lines) and *O*-linked (HPA, solid lines) glycans on Jurkat cells treated with **1-68A** (closed square) or **2-68A** (closed diamond).

(B) Evaluation of apoptosis by fluorescein isothiocyanate (FITC)-labeled Annexin-V staining of Jurkat cells treated with **1-68A** (closed square) or **2-68A** (closed diamond).

(C) Lectin staining of *N*-linked (Con A) and *O*-linked (HPA) glycans on Jurkat cells treated with doxorubicin (10 μM) or campothecin (10 μM).

(D) Evaluation of apoptosis by FITC-labeled Annexin-V staining of Jurkat cells treated with doxorubicin (10 μM) or campothecin (10 μM). MFI, mean fluorescence intensity of the total cell population. Each point on the graph represents the average of duplicates; bars represent the high and low values.

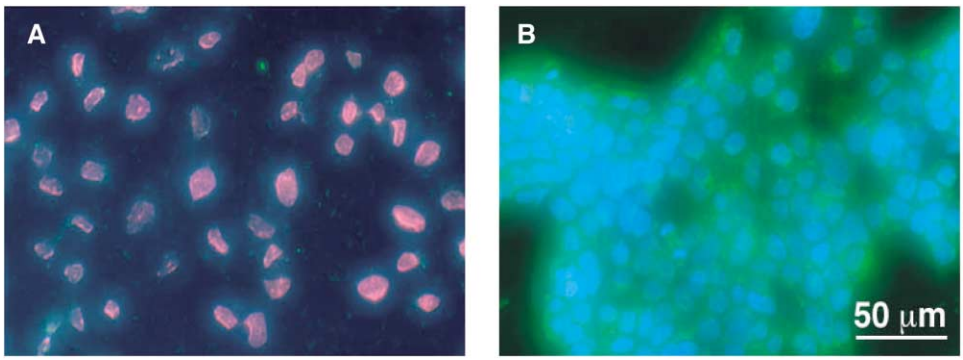

Figure 6. Fluorescence Microscopy Analysis of HEK 293T Cells for *O*-Linked Glycosylation and Apoptosis

(A) Cells treated with 100 μM **1-68A**.

(B) Cells treated with DMSO alone. Green, FITC-jacalin staining; blue, nuclei counterstain with Hoechst 33342; red, TUNEL staining. Scale bar applies to both images.

on human embryonic kidney (HEK) 293T cells. In this case, *O*-linked glycans on the cell surface were monitored by staining with jacalin, a lectin that binds core 1 structures (Galβ1,3-GalNAcα1-Ser/Thr) [63]. To evaluate apoptosis in HEK cells, TUNEL staining for DNA fragmentation was performed [64]. As shown in Figure 6A, **1-68A** inhibits jacalin staining at 100 μM and increases TUNEL staining compared to untreated HEK cells (Figure 6B). Thus, **1-68A** appears to block *O*-linked glycosylation and induce apoptosis in HEK cells as well as in Jurkat cells.

Significance

Chemical tools for studying *O*-linked glycosylation would facilitate functional studies of this critical post-translational modification. Toward this end, we sought inhibitors of the ppGalNAcTs that initiate *O*-linked glycosylation. Two compounds were identified from a uridine-based library using a novel high-throughput ELLA. They were competitive with respect to UDP-GalNAc with K_I values of approximately 8 μM and did not inhibit other enzymes such as β1-4GalT or α1-3GalT. The discovery of these inhibitors further validates the uridine-based library as a source of lead compounds for UDP-sugar utilizing enzymes. The 2,3,4-trihydroxybenzene motif present in both compounds is reminiscent of a monosaccharide and contributes significantly to binding. It is notable that the compounds bind with higher affinity than UDP-GalNAc without charged moieties that mimic the pyrophosphate group, which has been a major challenge in glycosyltransferase inhibitor design [65].

The compounds disrupted *O*-linked glycosylation in cells while also inducing apoptosis. Experiments are currently underway to dissect the relationship of these effects. It is worth noting that the compounds exhibit cellular effects despite their polar nature. This suggests they have a mechanism to enter cells, either by diffusion through membranes or by active uptake. It is possible that *O*-linked glycan disruption promotes apoptosis, similar to the toxic effects of the *N*-linked glycosylation inhibitor tunicamycin [41]. Alternatively, the compounds may induce apoptosis through a glycosylation-independent mechanism, resulting in abrogation of numerous metabolic pathways. However, the compounds did not affect *N*-linked glycosylation, suggesting a more specific mechanism. The compounds reported here are the first inhibitors of the ppGalNAcT family and provide a promising starting point for the development of more potent and selective inhibitors for individual ppGalNAcTs.

Experimental Procedures

Methyl 2-acetamido-2-deoxy-β-D-glucopyranoside (βOMeGlcNAc), pyruvate kinase, lactate dehydrogenase, phosphoenolpyruvate, NADH, and UDP-GalNAc were purchased from Sigma. HPA-HRP, FITC-HPA, FITC-Con A, and FITC-jacalin were from E-Y Laboratories. Transparent 96-well Reacti-Bind NeutrAvidin-coated plates and the HRP substrate 3,3′,5,5′-tetramethyl benzidine (TMB) were purchased from Pierce. Doxorubicin hydrochloride, campothecin, UDP-Gal, *N*-acetylactosamine (LacNAc), bovine β1-4GalT, and porcine α1-3GalT were purchased from Calbiochem. Aldehydes were purchased from Aldrich, ChemDiv, or ChemBlock as listed in the Supplemental Data at http://www.chembiol.com/cgi/content/full/11/3/337/DC1.

Enzyme assays were quantified using a Molecular Devices UV/Vis 96-well plate reader (SpectraMax 190). RP-HPLC was performed using a Rainin Dynamax SD-200 HPLC system with 230 nm detection on a Microsorb C-18 analytical column (4.6 × 250 mm) at a flow rate of 1 ml/min or a preparative column (25 × 250 mm) at a flow rate of 20 ml/min.

All ^{1}H and ^{13}C NMR spectra were recorded on a Bruker DRX 500 MHz NMR spectrometer. Chemical shifts are reported in ppm relative to tetramethylsilane. Coupling constants (*J*) are reported in Hz. Fast atom bombardment (FAB) and electrospray (ES) mass spectra were obtained at the UC Berkeley Mass Spectrometry Laboratory.

Jurkat cells were grown in RPMI-1640 media supplemented with 10% FCS, 100 units/ml penicillin, and 0.1 mg/ml streptomycin. HEK 293T cells were grown in MEM supplemented with 10% FCS, 2 mM L-glutamine, and Earle's BSS adjusted to contain 1.5 g/l sodium bicarbonate, 0.1 mM nonessential amino acids, and 1.0 mM sodium pyruvate. Cells were incubated in a 5% CO_2 humidified incubator at 37°C.

Solid-Phase Peptide Synthesis

The biotinylated peptides and glycopeptides were generated by standard Fmoc-based solid-phase peptide synthesis methods using N^{α}-Fmoc-Thr(Ac_3-α-D-GalNAc)-OH [53] as a glycosylated amino acid building block. Peptides were purified by RP-HPLC eluting with 10%–40% MeCN/H_2O with 0.1% TFA. *C-terminal biotinylated EA2*

(4): LRMS (ES): calculated for $C_{71}H_{119}N_{19}O_{25}S$ ($M+H^+$) 1670.9, found 1670.7. *C-terminal biotinylated EA2* (5)*: LRMS (ES): calculated for $C_{79}H_{132}N_{20}O_{30}S$ ($M+H^+$) 1874.1, found 1874.1. *MUC5AC*** LRMS (ES): calculated for $C_{79}H_{132}N_{19}O_{35}$ ($M+H^+$) 1907.0, found 954.5 ($M+2H^+$).

Expression of ppGalNAcTs

COS-7 cells were transiently transfected with plasmids encoding truncated secreted ppGalNAcTs 1–5, 7, 10, and 11 as previously described [19]. The crude conditioned medium was used as the enzyme source.

ELLA for ppGalNAcTs

Standard reaction conditions for ppGalNAcT assays were as follows. The reaction mixture contained the following components in a final volume of 25 μl: 10 mM $MnCl_2$, 40 mM sodium cacodylate, 40 mM β-mercaptoethanol, 0.1% Triton X-100 [pH 6.5], 5 μl of conditioned media, and various concentrations of EA2 peptide **4**, UDP-GalNAc, and inhibitor. All uridine-based compounds were dissolved in DMSO. We limited the concentration of DMSO in the reaction mixture to 2% (v/v), as higher concentrations decreased ppGalNAcT activity. For inhibitor assays, reaction mixtures for positive controls also contained 2% DMSO. Unless otherwise stated, inhibitor assays were performed using 20 μM UDP-GalNAc and 50 μM EA2 peptide **4**, the K_M values for both substrates. Reactions were incubated at 37°C and were terminated by the addition of 10 μl of 0.1 M EDTA. All experiments were performed in duplicate. Reaction rates were linear over the period monitored (20–30 min).

96-well NeutrAvidin-coated plates were prewashed 3 times with 200 μl of wash buffer (25 mM Tris, 150 mM NaCl, 0.1% bovine serum albumin (BSA) (w/v), and 0.05% Tween (v/v) [pH 7.2]). Reactions were then transferred to the 96-well plates, incubated for 1 hr at rt, and subsequently washed 3 times with 200 μl of phosphate-buffered saline (PBS) containing 0.5% BSA and 0.05% Tween (pH 7.1). A 100 μl solution of HPA-HRP in standard PBS buffer (1 μg/ml, pH 7.4) was added and the reaction was incubated for 1 hr at rt. After 3 washes with 200 μl of PBS, bound HPA-HRP was quantified by the addition of 100 μl of TMB peroxide solution. The solutions were incubated for 5–15 min in the dark at rt. HRP activity was terminated by the addition of 50 μl of 2 N H_2SO_4, and the resulting solution was analyzed at 450 nm using a UV/Vis microtiter plate reader. The amount of product generated by the ppGalNAcT was extrapolated from absorbance values using an equation fit to the standard curve derived from Origin 6.1 software.

Radiolabel Capture Assay for rppGalNAcT-5, -7, and -10

Radiolabel capture assays using ^{14}C-labeled UDP-GalNAc were performed as previously described with various concentrations of **1-68A** or **2-68A** in 2% DMSO [26].

Continuous Assay for β1-4GalT and α1-3GalT Activity

The enzymatic reactions contained the following components in a final volume of 100 μl: 20 mM $MnCl_2$, 100 mM sodium cacodylate (pH 6.5), 5 U of pyruvate kinase, 5 U of lactate dehydrogenase, 2 mM PEP, 0.2 mM NADH with 0.4 mU of β1-4GalT, 1 mM βOMeGlcNAc, 25 μM UDP-Gal or 1.0 mU of α1-3GalT, 1 mM LacNAc, 100 μM UDP-Gal, and various concentrations of **1-68A** or **2-68A** in 2.5% DMSO. The reaction mixtures were incubated at 37°C for 10 min before the reaction was initiated by the addition of UDP-Gal. The change in absorbance was monitored over 20 min at 340 nm.

Resynthesis of 1-68A and 2-68A

The aldehyde (0.06 mmol) and the corresponding uridine analog (0.08 mmol) were stirred for 16 hr at rt in 1% AcOH/DMSO (0.6 ml) in the dark. RP-HPLC purification eluting with a gradient of 15%–80% MeCN/H_2O afforded compound **1-68A** (16 mg, 0.04 mmol) in 67% yield as an off-white solid and compound **2-68A** (18 mg, 0.04 mmol) in 67% yield as an off-white solid.

1-68A ^{1}H NMR (500 MHz, CD_3OD): δ 8.26 (s, 1), 7.74 (d, 1, J = 8.1), 6.73 (d, 1, J = 8.5), 6.42 (d, 1, J = 8.5), 5.88 (d, 1, J = 4.2), 5.64 (d, 1, J = 8.1), 4.47 (app d, 1, J = 12.5), 4.37 (app d, 1, J = 12.3), 4.21–4.16 (m, 3H). ^{13}C NMR (125 MHz, MeOD): δ 164.6, 151.6, 150.8, 148.3, 146.0, 140.8, 132.5, 121.0, 109.2, 107.3, 101.3, 89.8, 82.8, 73.8, 73.2, 69.8. HRMS (FAB): calculated for $C_{16}H_{17}N_3O_9$ ($M+H^+$) 396.1039, found 396.1043.

2-68A ^{1}H NMR (500 MHz, CD_3OD): δ 8.33 (s, 1), 7.60 (d, 1, J = 8.1), 6.73 (d, 1, J = 8.6), 6.41 (d, 1, J = 8.5), 5.70 (d, 1, J = 4.8), 5.60 (d, 1, J = 8.0), 4.63 (app s, 1), 4.21 (app t, 1, J = 5.0), 4.04–4.02 (m, 2), 3.65–3.54 (m, 2). ^{13}C NMR (125 MHz, MeOD): δ 171.1, 164.6, 153.0, 150.8, 148.6, 146.0, 141.8, 132.5, 121.2, 108.9, 107.5, 101.4, 91.0, 82.2, 73.2, 72.4, 70.8, 40.4. HRMS (FAB): calculated for $C_{18}H_{20}N_4O_{10}$ ($M+H^+$) 453.1253, found 453.1258.

Evaluation of 1-68A, 2-68A, Doxorubicin, and Campothecin in Jurkat Cells

Jurkat cells were seeded at 250,000 cells/well (determined by Coulter cell counter) in 12-well polystyrene tissue culture plates in 1.0 ml of media and treated with various concentrations of **1-68A** or **2-68A** from 50 mM DMSO stock solutions or doxorubicin or campothecin from 1 mM DMSO stock solutions. After 2 days, cells were harvested, washed twice with PBS buffer (PBS [pH 7.4], 0.1% FCS, 0.1% NaN_3 w/v), and stained with FITC-HPA (1 μg/ml) or FITC-Con A (5 μg/ml with 1 mM $CaCl_2$) in PBS (pH 7.4) in the dark for 1 hr at 4°C. Cells were washed twice with PBS buffer, resuspended in 300 μl of PBS buffer, and analyzed by flow cytometry (FacsCaliber, BD Instruments). Annexin-V staining was performed according to the manufacturer's protocols (Invitrogen).

Evaluation of 1-68A and 2-68A in HEK 293T Cells

HEK 293T cells were seeded at 20,000 cells/ml in a 24-well plate (Costar) fit with glass coverslips (Fisher). After 24 hr of incubation with 100 μM **1-68A**, cells were washed twice with PBS (pH 7.4) and fixed with 4% paraformaldehyde-PBS for 1 hr at rt. The cells were washed twice with PBS and incubated with permeabilization solution (0.1% Triton X-100 in 0.1% sodium citrate, freshly prepared) for 2 min on ice. After the cells were washed twice with PBS, 50 μl of TUNEL reaction mixture (1:10 dilution, Boehringer Mannheim) was added. The plate was covered with parafilm to avoid evaporative loss and incubated in a humidified atmosphere for 1 hr at 37°C in the dark. The cells were then rinsed three times with PBS and blocked with 2% BSA in PBST (PBS, 0.05% Tween 20) for 30 min at rt. Following one wash with PBS, the cells were incubated with 100 μl of FITC-jacalin (4 μg/ml in PBST) for 1 hr at 37°C in the dark. The cells were washed three times with PBS, counterstained with Hoechst 33342 (Molecular Probes), and mounted with Fluoromount-G aqueous medium (Electron Microscopy Sciences). Slides were analyzed by fluorescence microscopy (Zeiss, using Openlab software).

Supplemental Data

Supplemental Data include the complete list of compounds comprising the uridine library, detailed synthetic procedures, and experimental details for K_i and IC_{50} measurements. These materials can be found online at http://www.chembiol.com/cgi/content/full/11/3/337/DC1.

Acknowledgments

The Center for New Directions in Organic Synthesis is supported by Bristol-Myers Squibb as supporting member and Novartis as sponsoring member. H.C.H. thanks Dupont Pharmaceuticals and the Organic Division of the American Chemical Society for a graduate fellowship. C.Y. thanks the Beckman Scholars Program for an undergraduate fellowship. This research was supported by a grant to C.R.B. from the National Institutes of Health (GM66047).

Received: August 11, 2003
Revised: November 10, 2003
Accepted: December 12, 2003
Published: March 19, 2004

References

1. Roslyn, M.B., Revers, L., and Wilson, I.B.H. (1998). Protein Glycosylation (Boston: Kluwer Academic Publishers).
2. Van den Steen, P., Rudd, P.M., Dwek, R.A., and Opdenakker,

G. (1998). Concepts and principles of *O*-linked glycosylation. Crit. Rev. Biochem. Mol. Biol. *33*, 151–208.

3. Ten Hagen, K.G., Fritz, T.A., and Tabak, L.A. (2003). All in the family: the UDP-GalNAc:polypeptide *N*-acetylgalactosaminyltransferases. Glycobiology *13*, 1–16.
4. Brockhausen, I. (2000). Biosynthesis of the *O*-glycan chains of mucins and mucin-type glycoproteins. In Carbohydrates in Chemistry and Biology, Volume 3, B. Ernst, G.W. Hart, and P. Sinay, eds. (New York: Wiley-VCH), pp. 313–328.
5. Perez-Vilar, J., and Hill, R.L. (1999). The structure and assembly of secreted mucins. J. Biol. Chem. *274*, 31751–31754.
6. Lichtenberger, L.M. (1995). The hydrophobic barrier properties of gastrointestinal mucus. Annu. Rev. Physiol. *57*, 565–583.
7. Gendler, S.J., and Spicer, A.P. (1995). Epithelial mucin genes. Annu. Rev. Physiol. *57*, 607–634.
8. Tabak, L.A. (1995). In defense of the oral cavity: structure, biosynthesis, and function of salivary mucins. Annu. Rev. Physiol. *57*, 547–564.
9. Lasky, L.A. (1995). Selectin-carbohydrate interactions and the initiation of the inflammatory response. Annu. Rev. Biochem. *64*, 113–139.
10. Tsuboi, S., and Fukuda, M. (2001). Roles of *O*-linked oligosaccharides in immune responses. Bioessays *23*, 46–53.
11. Taylor-Papadimitriou, J., Burchell, J., Miles, D.W., and Dalziel, M. (1999). MUC1 and cancer. Biochim. Biophys. Acta *1455*, 301–313.
12. Kornfeld, R., and Kornfeld, S. (1985). Assembly of asparagine-linked oligosaccharides. Annu. Rev. Biochem. *54*, 631–664.
13. Helenius, A., and Aebi, M. (2001). Intracellular functions of *N*-linked glycans. Science *291*, 2364–2369.
14. Hagen, F.K., Van Wuyckhuyse, B., and Tabak, L.A. (1993). Purification, cloning, and expression of a bovine UDP-GalNAc: polypeptide *N*-acetyl-galactosaminyltransferase. J. Biol. Chem. *268*, 18960–18965.
15. Homa, F.L., Hollander, T., Lehman, D.J., Thomsen, D.R., and Elhammer, A.P. (1993). Isolation and expression of a cDNA clone encoding a bovine UDP-GalNAc:polypeptide *N*-acetylgalactosaminyltransferase. J. Biol. Chem. *268*, 12609–12616.
16. White, T., Bennett, E.P., Takio, K., Sørensen, T., Bonding, N., and Clausen, H. (1995). Purification and cDNA cloning of a human UDP-*N*-acetyl-α-D-galactosamine:polypeptide *N*-acetylgalactosaminyltransferase. J. Biol. Chem. *270*, 24156–24165.
17. Bennett, E.P., Hassan, H., and Clausen, H. (1996). cDNA cloning and expression of a novel human UDP-*N*-acetyl-α-D-galactosamine. Polypeptide *N*-acetylgalactosaminyltransferase, GalNAc-T3. J. Biol. Chem. *271*, 17006–17012.
18. Zara, J., Hagen, F.K., Ten Hagen, K.G., Van Wuyckhuyse, B.C., and Tabak, L.A. (1996). Cloning and expression of mouse UDP-GalNAc:polypeptide *N*-acetylgalactosaminyltransferase-T3. Biochem. Biophys. Res. Commun. *228*, 38–44.
19. Hagen, F.K., Hagen, K.G., Beres, T.M., Balys, M.M., VanWuyckhuyse, B.C., and Tabak, L.A. (1997). cDNA cloning and expression of a novel UDP-*N*-acetyl-D-galactosamine:polypeptide *N*-acetylgalactosaminyltransferase. J. Biol. Chem. *272*, 13843–13848.
20. Ten Hagen, K.G., Hagen, F.K., Balys, M.M., Beres, T.M., Van Wuyckhuyse, B., and Tabak, L.A. (1998). Cloning and expression of a novel, tissue specifically expressed member of the UDP-GalNAc:polypeptide N-acetylgalactosaminyltransferase family. J. Biol. Chem. *273*, 27749–27754.
21. Bennett, E.P., Hassan, H., Mandel, U., Hollingsworth, M.A., Akisawa, N., Ikematsu, Y., Merkx, G., van Kessel, A.G., Olofsson, S., and Clausen, H. (1999). Cloning and characterization of a close homologue of human UDP-*N*-acetyl-α-D-galactosamine: polypeptide *N*-acetylgalactosaminyltransferase-T3, designated GalNAc-T6. Evidence for genetic but not functional redundancy. J. Biol. Chem. *274*, 25362–25370.
22. Ten Hagen, K.G., Tetaert, D., Hagen, F.K., Richet, C., Beres, T.M., Gagnon, J., Balys, M.M., VanWuyckhuyse, B., Bedi, G.S., Degand, P., et al. (1999). Characterization of a UDP-GalNAc: polypeptide *N*-acetylgalactosaminyltransferase that displays glycopeptide *N*-acetylgalactosaminyltransferase activity. J. Biol. Chem. *274*, 27867–27874.
23. Bennett, E.P., Hassan, H., Hollingsworth, M.A., and Clausen, H. (1999). A novel human UDP-*N*-acetyl-D-galactosamine:polypeptide *N*-acetylgalactosaminyltransferase, GalNAc-T7, with specificity for partial GalNAc-glycosylated acceptor substrates. FEBS Lett. *460*, 226–230.
24. White, K.E., Lorenz, B., Evans, W.E., Meitinger, T., Strom, T.M., and Econs, M.J. (2000). Molecular cloning of a novel human UDP-GalNAc: polypeptide *N*-acetylgalactosaminyltransferase, GalNAc-T8, and analysis as a candidate autosomal dominant hypophosphatemic rickets (ADHR) gene. Gene *246*, 347–356.
25. Toba, S., Tenno, M., Konishi, M., Mikami, T., Itoh, N., and Kurosaka, A. (2000). Brain-specific expression of a novel human UDP-GalNAc: polypeptide *N*-acetylgalactosaminyltransferase (GalNAc-T9). Biochim. Biophys. Acta *1493*, 264–268.
26. Ten Hagen, K.G., Bedi, G.S., Tetaert, D., Kingsley, P.D., Hagen, F.K., Balys, M.M., Beres, T.M., Degand, P., and Tabak, L.A. (2001). Cloning and characterization of a ninth member of the UDP-GalNAc:polypeptide *N*-acetylgalactosaminyltransferase family, ppGaNTase-T9. J. Biol. Chem. *276*, 17395–17404.
27. Ten Hagen, K.G., and Tran, D.T. (2002). A UDP-GalNAc:polypeptide *N*-acetylgalactosaminyltransferase is essential for viability in *Drosophila melanogaster*. J. Biol. Chem. *277*, 22616–22622.
28. Schwientek, T., Bennett, E.P., Flores, C., Thacker, J., Hollmann, M., Reis, C.A., Behrens, J., Mandel, U., Keck, B., Schafer, M.A., et al. (2002). Functional conservation of subfamilies of putative UDP-*N*-acetylgalactosamine:polypeptide *N*-acetylgalactosaminyltransferases in *Drosophila*, *Caenorhabditis elegans*, and mammals. One subfamily composed of l(2)35Aa is essential in *Drosophila*. J. Biol. Chem. *277*, 22623–22638.
29. Guo, J.M., Zhang, Y., Cheng, L., Iwasaki, H., Wang, H., Kubota, T., Tachibana, K., and Narimatsu, H. (2002). Molecular cloning and characterization of a novel member of the UDP-GalNAc: polypeptide *N*-acetylgalactosaminyltransferase family, pp-GalNAc-T12. FEBS Lett. *524*, 211–218.
30. Zhang, Y., Iwasaki, H., Wang, H., Kudo, T., Kalka, T.B., Hennet, T., Kubota, T., Cheng, L., Inaba, N., Gotoh, M., et al. (2003). Cloning and characterization of a new human UDP-*N*-acetyl-α-D-galactosamine:polypeptide *N*-acetylgalactosaminyltransferase, designated pp-GalNAc-T13, that is specifically expressed in neurons and synthesizes GalNAc α-serine/threonine antigen. J. Biol. Chem. *278*, 573–584.
31. Wang, H., Tachibana, K., Zhang, Y., Iwasaki, H., Kameyama, A., Cheng, L., Guo, J., Hiruma, T., Togayachi, A., Kudo, T., et al. (2003). Cloning and characterization of a novel UDP-GalNAc: polypeptide *N*-acetylgalactosaminyltransferase, pp-GalNAc-T14. Biochem. Biophys. Res. Commun. *300*, 738–744.
32. Ten Hagen, K.G., Tran, D.T., Gerken, T.A., Stein, D.S., and Zhang, Z. (2003). Functional characterization and expression analysis of members of the UDP-GalNAc:polypeptide *N*-acetylgalactosaminyltransferase family from *Drosophila melanogaster*. J. Biol. Chem. *278*, 35039–35048.
33. Wojczyk, B.S., Stwora-Wojczyk, M.M., Hagen, F.K., Striepen, B., Hang, H.C., Bertozzi, C.R., Roos, D.S., and Spitalnik, S.L. (2003). cDNA cloning and expression of UDP-*N*-acetyl-D-galactosamine:polypeptide *N*-acetylgalactosaminyltransferase T1 from *Toxoplasma gondii*. Mol. Biochem. Parasitol. *131*, 93–107.
34. Young, W.W., Jr., Holcomb, D.R., Ten Hagen, K.G., and Tabak, L.A. (2003). Expression of UDP-GalNAc:polypeptide *N*-acetylgalactosaminyltransferase isoforms in murine tissues determined by real-time PCR: a new view of a large family. Glycobiology *13*, 549–557.
35. Kingsley, P.D., Hagen, K.G., Maltby, K.M., Zara, J., and Tabak, L.A. (2000). Diverse spatial expression patterns of UDP-GalNAc:polypeptide *N*-acetylgalactosaminyl-transferase family member mRNAs during mouse development. Glycobiology *10*, 1317–1323.
36. Hassan, H., Bennet, E.P., Mandel, U., Hollingsworth, M.A., and Clausen, H. (2000). Control of mucin-type *O*-glycosylation: *O*-glycan occupancy is directed by substrate specificities of polypeptide GalNAc-transferases. In Carbohydrates in Chemistry and Biology, Volume 3, B. Ernst, G.W. Hart, and P. Sinay, eds. (New York: Wiley-VCH), pp. 273–292.
37. Elhammer, A.P., Kézdy, F.J., and Kurosaka, A. (1999). The acceptor specificity of UDP-GalNAc:polypeptide *N*-acetylgalactosaminyltransferases. Glycoconj. J. *16*, 171–180.

38. Imperiali, B. (1997). Protein glycosylation: the clash of the Titans. Acc. Chem. Res. *30*, 452–459.
39. Hansen, J.E., Lund, O., Tolstrup, N., Gooley, A.A., Williams, K.L., and Brunak, S. (1998). NetOglyc: prediction of mucin type *O*-glycosylation sites based on sequence context and surface accessibility. Glycoconj. J. *15*, 115–130.
40. Kirnarsky, L., Nomoto, M., Ikematsu, Y., Hassan, H., Bennett, E.P., Cerny, R.L., Clausen, H., Hollingsworth, M.A., and Sherman, S. (1998). Structural analysis of peptide substrates for mucin-type *O*-glycosylation. Biochemistry *37*, 12811–12817.
41. Elbein, A.D. (1987). Inhibitors of the biosynthesis and processing of *N*-linked oligosaccharide chains. Annu. Rev. Biochem. *56*, 497–534.
42. Peluso, S., de L. Ufret, M., O'Reilly, M.K., and Imperiali, B. (2002). Neoglycopeptides as inhibitors of oligosaccharyl transferase. Insight into negotiating product inhibition. Chem. Biol. *9*, 1323–1328.
43. Eason, P.D., and Imperiali, B. (1999). A potent oligosaccharyl transferase inhibitor that crosses the intracellular endoplasmic reticulum membrane. Biochemistry *38*, 5430–5437.
44. Kuan, S.F., Byrd, J.C., Basbaum, C., and Kim, Y.S. (1989). Inhibition of mucin glycosylation by aryl-*N*-acetyl-α-galactosaminides in human colon cancer cells. J. Biol. Chem. *264*, 19271–19277.
45. Sarkar, A.K., Fritz, T.A., Taylor, W.H., and Esko, J.D. (1995). Disaccharide uptake and priming in animal cells—inhibition of sialyl Lewis X by acetylated Gal-β1–4GlcNAc-β*O*-naphthalenemethanol. Proc. Natl. Acad. Sci. USA *92*, 3323–3327.
46. Sarkar, A.K., Rostand, K.S., Jain, R.K., Matta, K.L., and Esko, J.D. (1997). Fucosylation of disaccharide precursors of sialyl Lewis(X) inhibit selectin-mediated cell adhesion. J. Biol. Chem. *272*, 25608–25616.
47. Brown, J.R., Fuster, M.M., Whisenant, T., and Esko, J.D. (2003). Expression patterns of α2,3-sialyltransferases and α1,3-fucosyltransferases determine the mode of sialyl Lewis X inhibition by disaccharide decoys. J. Biol. Chem. *278*, 23352–23359.
48. Fuster, M.M., Brown, J.R., Wang, L., and Esko, J.D. (2003). A disaccharide precursor of sialyl Lewis X inhibits metastatic potential of tumor cells. Cancer Res. *63*, 2775–2781.
49. Winans, K.A., and Bertozzi, C.R. (2002). An inhibitor of the human UDP-GlcNAc 4-epimerase identified from a uridine-based library: a strategy to inhibit *O*-linked glycosylation. Chem. Biol. *9*, 113–129.
50. Scherman, M.S., Winans, K.A., Stern, R.J., Jones, V., Bertozzi, C.R., and McNeil, M.R. (2003). Drug targeting *Mycobacterium tuberculosis* cell wall synthesis: development of a microtiter plate-based screen for UDP-galactopyranose mutase and identification of an inhibitor from a uridine-based library. Antimicrob. Agents Chemother. *47*, 378–382.
51. Albone, E.F., Hagen, F.K., VanWuyckhuyse, B.C., and Tabak, L.A. (1994). Molecular cloning of a rat submandibular gland apomucin. J. Biol. Chem. *269*, 16845–16852.
52. Hammarstrom, S., Murphy, L.A., Goldstein, I.J., and Etzler, M.E. (1977). Carbohydrate binding specificity of four *N*-acetyl-D-galactosamine-"specific" lectins: *Helix pomatia* A hemagglutinin, soy bean agglutinin, lima bean lectin, and *Dolichos biflorus* lectin. Biochemistry *16*, 2750–2755.
53. Winans, K.A., King, D.S., Rao, V.R., and Bertozzi, C.R. (1999). A chemically synthesized version of the insect antibacterial glycopeptide, diptericin, disrupts bacterial membrane integrity. Biochemistry *38*, 11700–11710.
54. Wragg, S., Hagen, F.K., and Tabak, L.A. (1995). Kinetic analysis of a recombinant UDP-*N*-acetyl-D-galactosamine: polypeptide *N*-acetylgalactosaminyltransferase. J. Biol. Chem. *270*, 16947–16954.
55. Schanbacher, F.L., and Ebner, K.E. (1970). Galactosyltransferase acceptor specificity of the lactose synthetase A protein. J. Biol. Chem. *245*, 5057–5061.
56. Sharma, A., Okabe, J., Birch, P., McClellan, S.B., Martin, M.J., Platt, J.L., and Logan, J.S. (1996). Reduction in the level of Gal(α1,3)Gal in transgenic mice and pigs by the expression of an α(1,2)fucosyltransferase. Proc. Natl. Acad. Sci. USA *93*, 7190–7195.
57. Fitzgerald, D.K., Colvin, B., Mawal, R., and Ebner, K.E. (1970). Enzymic assay for galactosyl transferase activity of lactose synthetase and α-lactalbumin in purified and crude systems. Anal. Biochem. *36*, 43–61.
58. Piller, V., Piller, F., and Fukuda, M. (1990). Biosynthesis of truncated *O*-glycans in the T cell line Jurkat. Localization of *O*-glycan initiation. J. Biol. Chem. *265*, 9264–9271.
59. Baenziger, J.U., and Fiete, D. (1979). Structural determinants of concanavalin A specificity for oligosaccharides. J. Biol. Chem. *254*, 2400–2407.
60. Boersma, A.W., Nooter, K., Oostrum, R.G., and Stoter, G. (1996). Quantification of apoptotic cells with fluorescein isothiocyanate-labeled annexin V in chinese hamster ovary cell cultures treated with cisplatin. Cytometry *24*, 123–130.
61. A'Hern, R.P., and Gore, M.E. (1995). Impact of doxorubicin on survival in advanced ovarian cancer. J. Clin. Oncol. *13*, 726–732.
62. Staron, K., Kowalska-Loth, B., and Szumiel, I. (1994). The sensitivity to camptothecin of DNA topoisomerase I in L5178Y-S lymphoma cells. Carcinogenesis *15*, 2953–2955.
63. Sankaranarayanan, R., Sekar, K., Banerjee, R., Sharma, V., Surolia, A., and Vijayan, M. (1996). A novel mode of carbohydrate recognition in jacalin, a *Moraceae* plant lectin with a β-prism fold. Nat. Struct. Biol. *3*, 596–603.
64. Gavrieli, Y., Sherman, Y., and Ben-Sasson, S.A. (1992). Identification of programmed cell death in situ via specific labeling of nuclear DNA fragmentation. J. Cell Biol. *119*, 493–501.
65. Qian, X., and Palcic, M.M. (2000). Glycosyltransferase inhibitors. In Carbohydrates in Chemistry and Biology, Volume 3, B. Ernst, G.W. Hart, and P. Sinay, eds. (New York: Wiley-VCH), pp. 293–312.